Bull. Mater. Sci., Vol. 34, No. 5, August 2011, pp. 1127–1135. © Indian Academy of Sciences.

Catalytic oxidation of cyclohexane to cyclohexanone and cyclohexanol by *tert*-butyl hydroperoxide over Pt/oxide catalysts

I REKKAB-HAMMOUMRAOUI, A CHOUKCHOU-BRAHAM*, L PIRAULT-ROY† and C KAPPENSTEIN†

Laboratoire de Catalyse et Synthèse en Chimie Organique, Faculté des Sciences, Université A. Belkaid, B.P. 119 Tlemcen 13000, Algeria

†LACCO UMR CNRS 6503, Laboratoire de Catalyse en Chimie Organique, Faculté des Sciences, 86022 Poitiers Cedex, France

MS received 6 November 2010; revised 2 March 2011

Abstract. Heterogeneous oxidation of cyclohexane with tertiobutyl hydroperoxide was carried out on Pt/oxide (Al_2O_3, TiO_2 and ZrO_2) catalysts in the presence of different solvents (acetic acid and acetonitrile). The catalysts were prepared using $Pt(NH_3)_2(NO_2)_2$ as a precursor and characterized by chemical analysis using the ICP–AES method, XRD, TEM, FTIR and BET surface area determination. The oxidation reaction was carried out at 70°C under atmospheric pressure. The results showed the catalytic performance of Pt/Al_2O_3 as being very high in terms of turnover frequency.

Keywords. Oxidation; cyclohexane; platinum; TBHP; cyclohexanol; cyclohexanone.

1. Introduction

A mixture of cyclohexanone and cyclohexanol known as K/A oil is obtained by cyclohexane oxidation. These two compounds are important intermediates in the manufacture of nylon-6 and nylon-6–6 which have become important reference materials in the industrial production of polymers, and the demand has expanded over the last few years. The industrial scale preparation of cyclohexanol and cyclohexanone is carried out by oxidation of cyclohexane or by hydrogenation of phenol (Schuchardt *et al* 1993, 2001; Lu *et al* 2005). The earlier process is carried out at around 150°C and 1–2 MPa pressure, employing metal cobalt salt or metal-boric acid as homogeneous catalyst worldwide. The drawback of this process is that the oxidation must be operated in 3–6% conversion of cyclohexane to maintain a high selectivity (75–80%) for the K/A oil (Ingold 1989; Sawatari *et al* 2001). Many attempts have been made to synthesize more efficient catalysts for the oxidation of cyclohexane. Bellifa *et al* (2006) used a V_2O_5–TiO_2 catalyst which resulted in an 8% conversion and a 76% selectivity to cyclohexanol using acetic acid as solvent and acetone as initiator. Copper (II) complexes were used with H_2O_2 to give a total yield of 68·9% of cyclohexanol, cyclohexanone and other products in 24 h (Silva *et al* 2007). The use of Co_3O_4 nanocrystals gave a 7·6% conversion yielding cyclohexanol and cyclohexanone at 120°C in 6 h with molecular oxygen (Zhou *et al* 2005). A chromium containing complex, CrCoAPO–5(CH_3COOH) (Masters *et al* 2001) gave a 50% conversion, yielding 55%, 8%, 15% and 22% selectivities towards cyclohexanol, cyclohexanone, adipic acid and others, respectively at 115°C and 1 MPa of oxygen. The Co/ZSM-5 catalyst (Yuan *et al* 2006) was reported to give about 10% mol conversion and 97% selectivity to cyclohexanone and cyclohexanol at 120°C and 1·0 MPa pressure of O_2. A zirconium complex bonded to modify carbamate silica gel gave a product distribution ratio of 6·6:1 of cyclohexanol/cyclohexene mixture with 21% conversion at 200°C (Anisia and Kumar 2004). Titanium silicate (Reddy and Sivasankar 1991) gave 27·8 mol % conversion with selectivities of 44 mol %, 45 mol % and 11 mol % towards cyclohexanol, cyclohexanone and other products, respectively in a 5 h reaction at 100°C with hydrogen peroxide as oxidant. The Au/Al_2O_3 system using molecular oxygen in a solvent free system resulted in 12·6% conversion with a selectivity of 52·6% for cyclohexanol and 32·1% for cyclohexanone (Xu *et al* 2007). A similar use of Au/MCM-41 with oxygen resulted in 19% conversion with 21·3% and 6% selectivity towards cyclohexanol, cyclohexanone and other products, respectively (Lu *et al* 2004). Ebadi *et al* (2007) reported Fe, Mn and CoPc supported on gamma–alumina as catalysts for aerobic oxidation of cyclohexane in the gas phase under atmospheric pressure. They obtained 38% of selectivity for cyclohexanol and cyclohexanone with 29% conversion of cyclohexane. Recently, Yao *et al* (2006) reported a conversion of 95% over Ce–MCM-41 at 100°C over 12 h; this gave 82% selectivity to cyclohexanol. Sakthivel and Selvam (2002) reported

*Author for correspondence (cba@mail.univ-tlemcen.dz)

a conversion of 99% yielding 82% and 6·6% selectivities towards cyclohexanol, and cyclohexanone, respectively using calcined Cr–MCM-41 catalyst. Here again, the reaction was carried out at 100°C and over a 12 h duration. This is by far the most promising catalyst reported in the literature to date. However, the long reaction time and high temperature are grounds for further improvement, and it is still difficult to apply these technologies to industrial processes.

Platinum catalyst, Pt/C, in the presence of $H_3PMo_{12}O_{40}\cdot 14H_2O$, an heteropoly compound, representing active catalytic systems for cyclohexane oxidation with a mixture of O_2 and H_2 gases and a selectivity of 64·8 μmol for cyclohexanol and 16·9 μmol for cyclohexanone was reported (Kuznetsova *et al* 2003). Radic *et al* (2004) conducted studies on the complete oxidation of hexane and toluene in the presence of Pt/Al_2O_3. They demonstrated that the specific activity of hydrocarbons oxidation in the presence of catalysts based on supported platinum and palladium is known to depend on the size of metal crystallites (Carballo *et al* 1978; Kobayashi *et al* 1988; Marecot *et al* 1994; Labalme *et al* 1996; Pliangos *et al* 1997; Papaefthimiou *et al* 1998; Garetto and Apesteguia 2000). The development of specific activities based on the particle size of noble metals has been attributed to morphological effects of the metals and not to their chemical effects. The TOF of supported noble metals improved while increasing their size.

Here, we report Pt/oxides (Al_2O_3, TiO_2 and ZrO_2) catalysts which show satisfactory conversion to the cyclohexane oxidation and selectivity of cyclohexanol and cyclohexanone using tertiobutyl hydroperoxide in CH_3CN and CH_3COOH as solvents.

2. Experimental

2.1 *Catalyst preparation*

The following supports, Al_2O_3 (Oxid C Degussa), TiO_2 (Titandioxid Degussa), ZrO_2 (Aldrich), of commercial grade were purchased in the form of nanopowder (in the range, 10–50 nm). They required further treatment before the impregnation of the metal precursors. The supports were mixed with water (200 mL H_2O for 100 g of support) in order to form a paste. The latter was dried overnight at 120°C, and then sieved to retain only the particles having a diameter ranging between 0·1 and 0·25 nm. Then the support underwent calcination at 400°C under oxidative flow (20% O_2, 80% Ar, 60 mL/min) during 4 h.

An aqueous solution of Pt $(NH_3)_2(NO_2)_2$ (Alfa Aesar) was then impregnated on these oxides in order to obtain 1 and 5% wt. of platinum catalyst. After solvent evaporation, the solids were dried at 120°C overnight, then calcined at 400°C for 4 h under oxidative atmosphere (Ar: 48 mL/min – O_2: 12 mL/min). Finally, the solids were reduced in H_2 (60 mL/min) at 400°C for 4 h.

2.2 *Characterization*

Chemical composition of the samples were analysed by inductively coupled plasma-atomic emission spectroscopy (ICP-AES) using an OPTIMA 2000 DV spectrometer.

Diffractograms of the catalysts were obtained by X-ray diffraction (XRD) experiments performed on a Siemens D5005 powder diffractometer using Cu Kα radiation (λ = 0·15186 nm) and a backmonochromator. XRD patterns were recorded using 2 s dwell time, 0·04° step size and a constant divergence slit of 18. Crystalline planes were identified by comparison with PDF standards from ICDD.

The N_2 adsorption–desorption measurements of supports were carried out at −196°C using Micromeritics Tristar. Surface areas of all the supports were calculated using Brunauer–Emmett–Teller method, whereas Barrett–Joyner–Halenda method was employed to get pore size distribution. Pore size distribution was obtained from desorption branch of isotherms.

The acidity of supports was characterized by pyridine adsorption followed by IR spectroscopy. IR spectra were recorded on a Nicolet Magna IR spectrometer using a thin wafer (16 mm in diameter, 10–15 mg·cm^{-2}) activated *in situ* in the IR cell under secondary vacuum (10^{-3} Pa) at 200°C for 2 h. Pyridine was adsorbed on the sample at 150°C. The IR spectra were recorded at room temperature after activation and pyridine thermodesorption under vacuum (10^{-3} Pa) for 1 h at 150°C. The total amounts of Lewis acid sites accessible to pyridine were quantified by the subtraction between P_{150} spectrum (spectrum of the catalyst after adsorption–desorption at 150°C of pyridine) and P_{ref} (spectrum of the catalyst before adsorption of pyridine). This technique allowed on one hand elimination of the solid intrinsic absorbance in the wavelength range studied, and on another hand the ignorance of the pyridine physisorption influence (below 150°C). Concentrations of Lewis acid sites able to retain pyridine adsorbed at 150°C were determined from the normalized absorbance areas of the band at 1455 cm^{-1} (PyL), using extinction coefficients previously determined. Spectra were also recorded after pyridine thermodesorption under vacuum (10^{-3} Pa) for 1 h at 250°C, 350°C and 450°C.

Electron microscopic studies of the catalysts were carried out on a JEOL 2000 FX instrument operating at 200 kV. Catalyst specimens for electron microscopy were prepared by grinding the powder samples in an agate mortar, suspending and sonicating them in ethanol, and placing a drop of the suspension on a holey carbon copper grid. After evaporation of the solvent, the specimens were introduced into the microscope column. The area distribution of particles was determined by counting a large number of particles (>500) on the TEM micrographs and by plotting n_i as a function of d_i (n_i is the number of particles within different intervals with given average diameters d_i). The mean surface diameter (Perkas *et al* 2005) of particles is then given by $d = \sum n_i d_i^3 / \sum n_i d_i^2$. The measurements were done

manually using the ImageJ program (Rasband and Image 1997–2005).

The chemisorption measurements were carried out in a glass volumetric catalyst system. Catalyst samples of ~0·2 g were placed into a reactor and reduced with pure H_2 for 2 h at 400°C. After evacuating the catalysts at the same temperature for 2 h, two adsorption isotherms (figure 1) were obtained at ambient temperature. The linear region of the first isotherm was extrapolated to zero pressure in order to calculate the amount of physisorbed and chemisorbed H_2 (HC_T). After an evacuation period of 1 h, the second isotherm of H_2 was obtained (HC_R). The same procedure (as the first isotherm) was used to calculate the amount of physisorbed species. The irreversibly held H_2 was calculated from the difference between the two values. A 1/1 H/Pt stoichiometry was assumed in order to calculate the metallic dispersion. From the platinum dispersion, the mean diameter of the platinum particles (d) was calculated using the formula:

$$d\ (\text{nm}) = \frac{5 \times 10^3}{\rho_{\text{Pt}} \times S_{\text{Pt}} \times D},$$

where ρ_{Pt} is the Pt density (21·4 g·cm^3), S_{Pt} the specific area of Pt (275 m^2 ·g^{-1}) and D the dispersion of platinum.

2.3 *Catalytic reactions*

The catalytic oxidation of cyclohexane with tertiobutyl hydroperoxide (TBHP) as the oxidant was carried out in a glass round-bottom flask with a magnetic stirrer and reflux condenser. First, commercial TBHP 70% in H_2O (Aldrich) was stirred with cyclohexane in order to perform a phase transfer from water to cyclohexane. In a typical reaction,

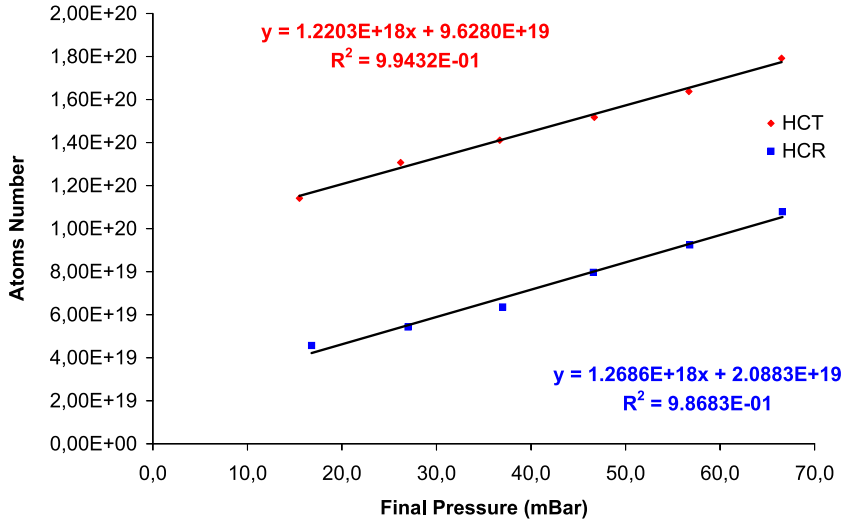

Figure 1. Example of hydrogen adsorption isotherms (HC_T) and (HC_R).

Table 1. Textural properties of catalysts and supports.

		Supports			
Catalysts	ICP (wt. %)	Lewis acidity (μmol g^{-1})	Surface area (m^{2}g^{-1})	Pore size (nm)	Pore volume (cm^{3}g^{-1})
Pt/Al_2O_3	5·06 1·02	150	95	31	0·72
Pt/ZrO_2	4·94 0·98	52	35	30	0·26
Pt/TiO_2	5·00 1·03	6	43	26	0·27

Table 2. Metallic accessibility and crystallite size for various catalysts.

Catalyst	Metal content (%)	Chemisorption		TEM	
		Dispersion (%)	Particle size[a] (nm)	Dispersion (%)	Particle size[b] (nm)
Pt/Al_2O_3	1·02	20	4·7	/	/
	5·06	28	3·3	29	3·2
Pt/ZrO_2	0·98	31	3·02	/	/
	4·94	42	2·2	54	1·7
Pt/TiO_2	1·03	60	1·5	/	/
	5·00	52	1·8	54	1·7

[a]Calculated upon the number of accessible Pt using cubic particle model with 5 accessible facets; [b]estimated from particle sizes using cubic particle model with 5 accessible facets.The surface area per Pt site (a_m) is taken as 8·08 $Å^2$.

60 mmol (6·5 mL) of cyclohexane and 60 mmol (8·5 mL) of oxidant (TBHP) were mixed in a closed Erlenmeyer flask and magnetically stirred for 24 h. The organic phase was then separated from the aqueous phase. In order to control the phase transfer, concentration of the remaining TBHP in the aqueous phase was determined by iodometric titration, and was found to be <10%. The solvent (50 mL) was then added to the TBHP–cyclohexane mixture. These reactants and solvent were introduced in a glass round-bottom flask and heated at 70°C under vigorous stirring. The catalyst (0·05 g) was subsequently added to the reaction mixture (time zero). The reaction products were identified by comparison with authentic products and the course of reactions was followed by gas chromatography (GC) using a Varian CP-3800 gas chromatograph equipped with a CP-WAX 52 CB column. A flame ionization detector (FID) was used and 0·5 µL of the sample was analysed. Before GC analysis, the remaining TBHP was decomposed by introducing an excess of triphenylphosphine (Aldrich). On the other hand, to control this remaining TBHP, an iodometric titration was performed at the end of the reaction (after 6 h) by testing the organic phase.

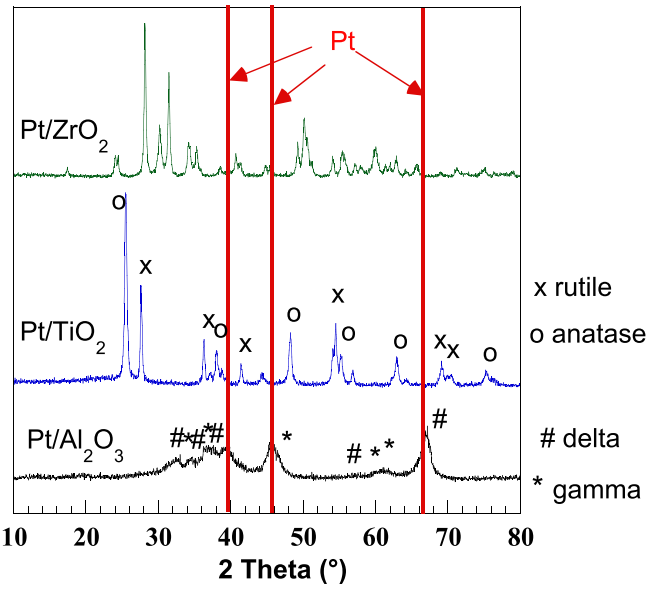

Figure 2. XRD patterns of catalysts.

3. Results and discussion

3.1 *Textural properties*

Table 1 shows textural properties of catalysts and supports. Al_2O_3 support displays the largest BET surface area (95 $m^2 \cdot g^{-1}$) and pore volume, whereas ZrO_2 has a lower BET area (35 $m^2 \cdot g^{-1}$) and has the same pore volume as that of TiO_2 which presents a BET area of 43 $m^2 \cdot g^{-1}$. These supports display the same pore size (30 nm). On the other hand, IR spectra of pyridine adsorption showed the presence of Lewis acid sites (1455 cm^{-1}) in all supports. We note the absence of characteristic bands of pyridine adsorption on Brønsted acid sites (formation of pyridinium ion leading to two adsorption bands at 1545 cm^{-1} and 1637 cm^{-1}). Al_2O_3 support is acidic (150 µmol·g^{-1} at 150°C) compared to ZrO_2 and TiO_2 which have 52 µmol·g^{-1} at 150°C and 6 µmol·g^{-1} at 150°C, respectively. As measured by ICP-AES, the platinum content in all catalysts is 1 or 5%.

3.2 *Metal dispersion*

The metal dispersion of catalysts was obtained by H_2 chemisorption at 25°C. The percentage dispersion of metallic Pt was calculated assuming an H/M atomic ratio (Corma *et al* 1997) of 1 as shown in table 2.

It is noteworthy to mention that the 5% Pt/Al_2O_3 catalyst gave lower dispersion than the 5% Pt/TiO_2, likely due to the acidic media. The Lewis acidity of the samples (table 1) decreases in the following order: $Al_2O_3 > ZrO_2 > TiO_2$. The smallest particle size was obtained for Pt/TiO_2 catalyst (1·8 nm) while the biggest corresponded to Pt/Al_2O_3

(3·3 nm). The deposited catalysts on ZrO_2 showed the formation of particles of ∼2 nm in size. This proved to be considerably smaller than the mesopore diameter, indicating that incorporation of the particles in the mesopores could readily occur. Additionally, the 1% Pt catalysts gave lower dispersion than the 5% Pt ones. By correlating the metal particle sizes to pore volumes, we can deduce that large particles are formed in the presence of Pt/Al_2O_3 (0·72 $cm^3\ g^{-1}$)

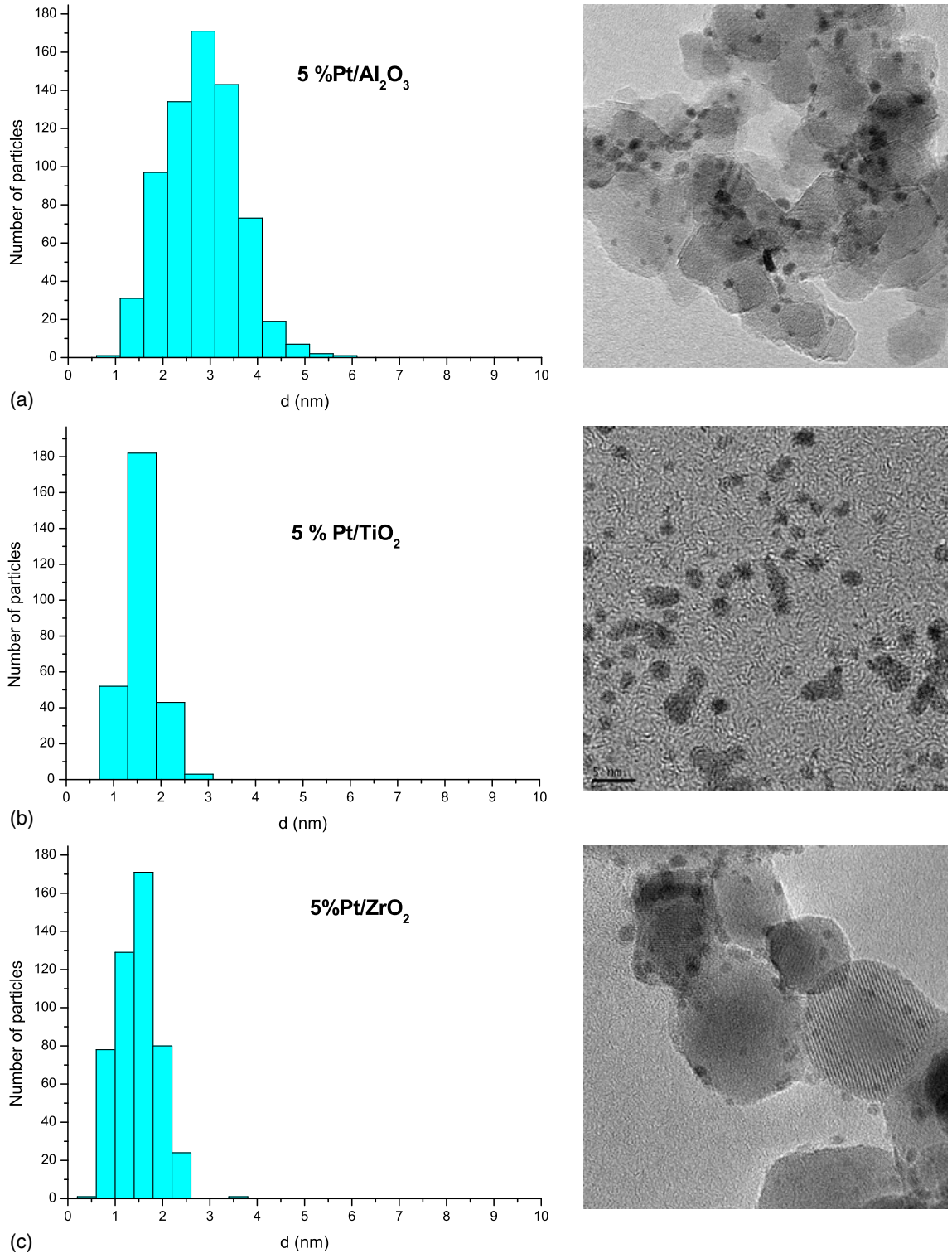

Figure 3. TEM photos of catalysts and particle size distribution: Pt/Al_2O_3 (**a**), Pt/TiO_2 (**b**) and Pt/ZrO_2 (**c**).

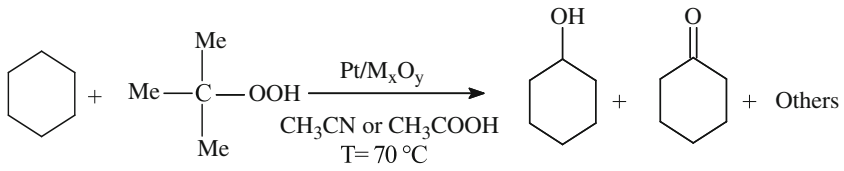

Scheme 1. Catalytic oxydation of cyclohexane to cyclohexanone and cyclohexanol.

Table 3. Oxidation of cyclohexane with different catalysts.

			Acetic acid				Acetonitrile			
				Selectivity (mmol)				Selectivity (mmol)		
Support	wt. (%)	*d* (nm)	TOF (h^{-1})	Ol	One	Others	TOF (h^{-1})	Ol	One	Others
Al_2O_3	5·06	3·34	782	2·8	0·7	13·54	481	0·5	0	10
	1·02	4·68	2830	2	0·56	6·32	1377	1·5	0	2·8
TiO_2	5·00	2·18	169	4	1·4	6·6	95	1	0·5	2·1
	1·03	1·56	793	0·92	0·45	7·63	520	0·4	0	4·4
ZrO_2	4·94	1·80	440	1·8	2	13·6	334	0·5	0	12·7
	0·98	3·02	1412	1	0·3	5·3	1155	0·4	0	5

C_6H_{12} = 6·5 mL; TBHP = 8·5 mL; solvent = 50 mL; catalyser = 0·05 g; t = 6 h; T = 70°C;
TOF = mole of converted cyclohexane per unit time per mole of dispersed platinum.

while smaller ones are formed in the presence of Pt/TiO_2 and Pt/ZrO_2 (0·27 cm^3 g^{-1}).

3.3 *XRD characterization*

All diffractograms (figure 2) confirm that metallic platinum is present in catalysts as a result of the reduction step and no platinum oxide is observed. Metallic Pt is indicated by peaks at 39·76°, 46·24° and 67·45° 2θ. Alumina-based catalyst shows two crystalline phases with sharper peaks, indicating that alumina is in δ and γ forms. The diffractogram of the supported catalyst on TiO_2 shows the two well known titanium oxide crystalline phases, viz. anatase and rutile, and only weak diffraction peaks of platinum are shown. Zirconia support is highly crystalline resulting in very intense peaks and the Pt metallics species can be seen as well.

3.4 *TEM characterization*

The TEM pictures of the prepared catalysts are shown in figure 3. The 5% Pt/Al_2O_3 catalyst sample was well dispersed with no indication of agglomeration of the Pt particles (figure 3a). The particle size was found to be in the range of 1·5–6 nm, the diameter being mostly 2–4 nm. The 5% Pt/TiO_2 had a narrow size distribution of particles in the range of 1–2·5 nm with a mean surface diameter of 1·73 nm (figure 3b). From the direct TEM micrographs (figure 3c), it may be noted that the ZrO_2 support had a more irregular morphology. It was coated by small particles of platinum. On the other hand, the TEM pictures of 5% Pt/ZrO_2 indicated showed particles in the range 1–2·5 nm but also larger particles of platinum up to 3·5 nm (figure 3c). Similar surface diameters of Pt particles (1·73 nm) are shown in 5% Pt/TiO_2 and 5%Pt/ZrO_2. The same particle sizes were obtained for catalysts based on TiO_2 and ZrO_2 by Perkas *et al* (2005). On the other hand, the crystallite sizes estimated by chemisorption of H_2 are the same which confirm the results (table 2).

3.5 *Cyclohexane oxidation*

Kinetic studies of the catalytic oxidation of cyclohexane with TBHP as oxidant, in acetonitrile or acetic acid as solvent at 70°C were performed on different samples. The desired products are cyclohexanol ($C_6H_{11}OH$), cyclohexanone ($C_6H_{10}O$) (scheme 1), but other products like cyclohexyl hydroperoxide, adipic acid, ester dicyclohexyl adipate, hexanolactone, and other esters (Zhou *et al* 2005), cyclohexyl acetate (Kumar *et al* 2009) did also form. In general, cyclohexyl hydroperoxide can be easily converted into cyclohexanol by reduction with a variety of reducing agents, thus increasing the yield of the target compounds. For this study, we focused on the selectivity towards olone only (cyclohexanol and cyclohexanone). The amount of the used catalyst was

0·05 g and the cyclohexane to TBHP mole ratio was (1:1). The results are shown in table 3.

In the preliminary experiments, a non-catalyzed oxidation reaction was carried out under typical reaction conditions and no oxidative products were formed.

Moreover, to check the impact of the supports on the cyclohexane oxidation reaction, we tested them as catalysts (figures 4–6). All supports exhibited conversions <15% and good selectivities (around 30%), as expected from the results of Bellifa *et al* (2006) and Zhao *et al* (2006). All the supports are active during the oxidation of cyclohexane but the presence of metal clearly improves the activity of the reaction. This improvement is not the same for all samples although the Pt content is the same and particle sizes are very close.

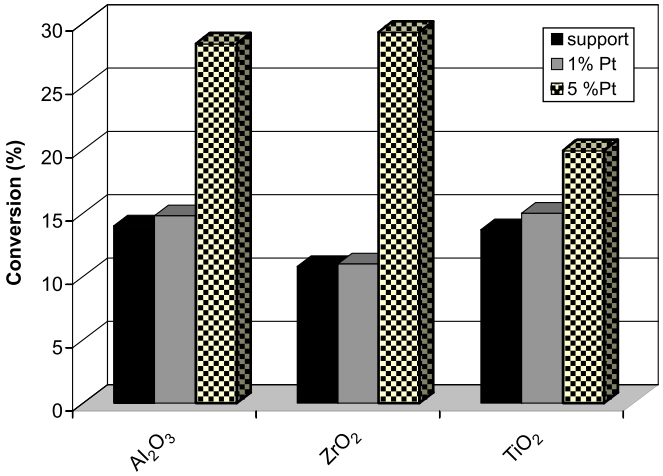

Figure 4. Effect of supports on activity of catalysts (C_6H_{12} = 60 mmol; TBHP = 60 mmol; acetic acid = 50 mL; catalyst = 0·05 g; t = 6 h; T = 70°C).

Cyclohexanol and cylohexanone selectivities increase with metal content. The 1% catalysts showed a modest increase compared to the 5% ones. So, we can assume that the support participates in the reaction via a functional mechanism (support and metal), as concluded by Wangcheng *et al* (2008).

The solvent usually determines the medium polarity and plays an important role in the activity of catalysts (Pires *et al* 2000), but the main action of solvent is still to facilitate homogeneity of immiscible liquid phase. No significant effect of solvent has been reported for cyclohexane oxidation. The effects of solvent on the catalytic activity of cyclohexane oxidation over Pt/M_xO_y are also depicted in table 3. In presence of acetic acid, cyclohexanol and cyclohexanone selectivities of alumina catalyst change a bit with the metal contents. We only observed an increase in the byproduct selectivity. It increases from 6·3 mmol for 1% to 13·5 mmol for 5%. The activity drops when the platinum content increases.

In the presence of acetonitrile, it is clear that platinum does not promote the formation of cyclohexanone. The cyclohexanol selectivity decreases when the platinum content increases from 1 to 5%. As with acetic acid, the activity decreases with an increase in platinum.

Comparing the two solvents, we find that the acetic acid leads to higher selectivities. Furthermore, high activities are obtained under acidic conditions compared to those obtained in acetonitrile medium, and they decrease when the platinum content increases. 1% Pt/TiO_2 did not give cyclohexanone in acetonitrile. Low cyclohexanol selectivity is obtained, however, the amount of byproducts is much greater. This means that platinum directs the reaction to other products other than oxidation to cyclohexanol and cyclohexanone. For contents of 5% platinum, cyclohexanone is produced. In the acid medium, 4 mmol of cyclohexanol and 1·4 mmol of

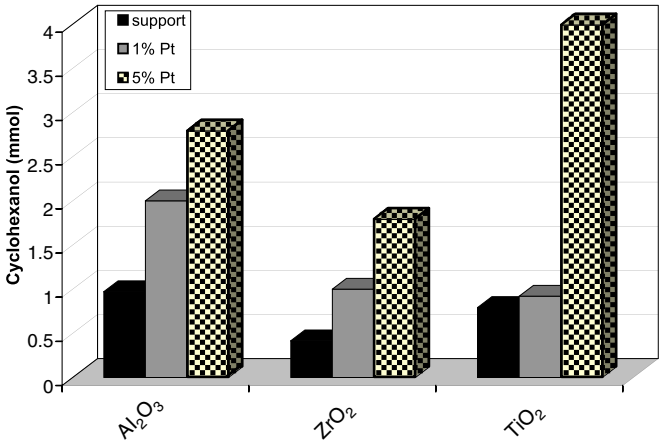

Figure 5. Selectivity of cyclohexanol as function of supports (C_6H_{12} = 60 mmol; TBHP = 60 mmol; acetic acid = 50 mL; catalyst = 0·05 g; t = 6 h; T = 70°C).

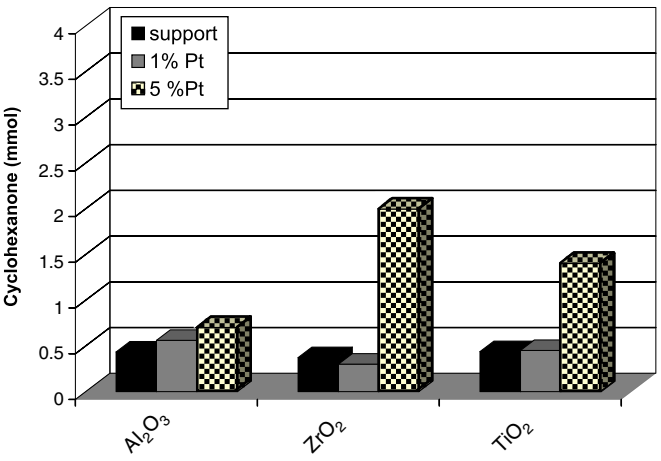

Figure 6. Selectivity of cyclohexanone as function of supports (C_6H_{12} = 60 mmol; TBHP = 60 mmol; acetic acid = 50 mL; catalyst = 0·05 g; t = 6 h; T = 70°C).

cyclohexanone are produced and the selectivity in products does not exceed 1 mmol. In acetonitrile medium, lower selectivities of olone mixtures (cyclohexanol + cyclohexanone) are obtained and the amount of byproducts becomes important.

Regarding the catalysts of platinum supported on zirconium oxide, the evolution of cyclohexanol selectivity with regard to the metal content is less pronounced in the presence of acetonitrile. Indeed, we observe no increase in selectivity when the platinum content increases and no production of cyclohexanone is visible. The formation of byproducts increases significantly with the platinum content to about 12·6 mmol in the presence of acetonitrile and 13·6 mmol in the presence of acetic acid. We can see that these catalysts lead mainly to products other than olone mixing.

Apparently, Pt/TiO_2 catalyst has the best performance in acetic acid. The higher selectivity of Pt/TiO_2 in acetic acid compared to acetonitrile may be explained in the same way as in Du *et al* (2009). As is known, enhancement of the activity by acetic acid in the oxidation of cyclohexane has been reported in the literature (Shulpin *et al* 1999; Sooknoi and Limtrakul 2002). In acetic acid, TBHP is stabler and diminishes the self-decomposition by forming peroxyacetic acid. Cyclohexane and TBHP are dissolved in acetic acid and the reaction products (cyclohexanol and cyclohexanone) are not only soluble in the reaction mixture but can also be displaced from the catalyst surface as they formed.

As listed in table 3, acetonitrile is not a perfect solvent for cyclohexane oxidation over Pt catalysts. The best catalytic performance was obtained in the presence of acetic acid which presents a turnover frequency (TOF) of 2830 h^{-1} over 1% Pt/Al_2O_3. Furthermore and surprisingly, the high TOF was attained over 1% Pt/oxides.

However, as the platinum loadings of our samples increased from 1 to 5%, both the conversion of cyclohexane and the total selectivity to the products increased, and a sharp decrease of the TOF value became evident at the same time. These effects are more likely caused by a decrease of highly active Pt particles since the particles grow bigger according to the TEM analysis.

4. Conclusions

Various oxide supported Pt catalysts were investigated for oxidation of cyclohexane with TBHP. The main conclusions are:

(I) XRD analysis showed that metallic platinum is present in catalysts and no oxide was observed.

(II) All the supports are active during oxidation of cyclohexane but the presence of metal clearly improves activity of the reaction.

(III) Activity depends on the acidity of the support or Pt particles size and can be ordered as follows:

$$Pt/Al_2O_3 > Pt/ZrO_2 > Pt/TiO_2.$$

(IV) Acetic acid as a solvent is better than acetonitrile, since acetic acid gave high conversion and high selectivity to cyclohexanol.

Acknowledgement

Authors thank the Algerian Ministry of Higher Education and Scientific Research for the fellowship funding in University of Poitiers, France.

References

Anisia K S and Kumar A 2004 *Appl. Catal. A: Gen*. **273** 193
Bellifa A, Lahcene D, Technar Y N, Choukchou-Braham A, Bachir R, Bedrane S and Kappenstein C 2006 *Appl. Catal. A: Gen*. **305** 1
Carballo L, Serrano C, Wolf E E and Carberry J 1978 *J. Catal*. **52** 507
Corma F, Sepulveda-Escribano A, Fierro J L and Rodriguez-Reinoso F 1997 *Appl. Catal. A: Gen*. **150** 165
Du Y, Xiong Y, Li J and Yang X 2009 *J. Mol. Catal. A: Chem*. **298** 12
Ebadi A, Safari N and Peyrovi M H 2007 *Appl. Catal. A: Gen*. **321** 135
Garetto T F and Apesteguia C R 2000 *Catal. Today* **62** 189
Ingold K U 1989 *Aldrichim. Acta* **22** 69
Kobayashi M, Kanno T, Konishi A and Takeda H 1988 *React. Kinet. Catal. Lett*. **37** 89
Kumar R, Sithambarama S and Suib S L 2009 *J. Catal*. **262** 304
Kuznetsova N I, Kirillova N V, Kuznetsova L I and Likholobov V A 2003 *J. Mol. Catal. A: Chem*. **204–205** 591
Labalme V, Garbowsky E, Ghilhaume N and Primet M 1996 *Appl. Catal. A: Gen*. **138** 93
Lu G, Zhao R, Qian G, Qi Y, Wang X and Suo J 2004 *Catal. Lett*. **97** 115
Lu G, Ji D, Qian G, Qi Y, Wang X and Suo J 2005 *Appl. Catal. A: Gen*. **280** 175
Marecot P, Fakche A, Kellali B, Mabilon G, Prigent M and Barbier J 1994 *Appl. Catal. B: Environ*. **3** 283
Masters A F, Beattie J K and Roa A L 2001 *Catal. Lett*. **75** 159
Papaefthimiou P, Ioannides T and Verykios X E 1998 *Appl. Catal. B: Environ*. **15** 75
Perkas N, Minh D P, Gallezot P, Gedanken A and Besson M 2005 *Appl. Catal. B: Environ*. **59** 121
Pires E L, Magalhaes J C and Schuchardt U 2000 *Appl. Catal. A: Gen*. **203** 231
Pliangos C, Yentekakis I V, Papadakis V G, Vayenas C G and Verykios X E 1997 *Appl. Catal. B: Environ*. **14** 161
Radic N, Grbic B and Terlecki-Baricevic A 2004 *Appl. Catal. B: Environ*. **50** 153
Rasband W and Image J 1997–2005 U.S. National Institutes of Health, Bethesda, MD, USA http://rsb.info.nih.gov/ij/
Reddy J S and Sivasanker S 1991 *Catal. Lett*. **11** 241
Sakthivel A and Selvam P 2002 *J. Catal*. **211** 134
Sawatari N, Yokota T, Sakaguchi S and Ishii Y 2001 *J. Org. Chem*. **66** 7889
Schuchardt U, Carvalho W A and Spinace E V 1993 *Synlett*. 713
Schuchardt U *et al* 2001 *Appl. Catal. A: Gen*. **211** 1
Shulpin G B, Fink G S and Smith J R 1999 *Tetrahedron* **55** 5345

Silva A C *et al* 2007 *Appl. Catal. A: Gen*. **317** 154
Sooknoi T and Limtrakul J 2002 *Appl. Catal. A: Gen*. **233** 227
Wangcheng Z, Guanzhong L, Yanglong G, Yun G, Yanqin W, Yunsong W, Zhigang Z and Xiaohui L 2008 *J. Rare Earths* **26** 515
Xu L X, He C H, Zhu M Q and Fang S 2007 *Catal. Lett*. **114** 202
Yao W, Chen Y, Min L, Fang H, Yan Z, Wang H and Wang J 2006 *J. Mol. Catal. A: Chem*. **246** 162
Yuan H X, Xia Q H, Zhan H J, Lu X H and Su K X 2006 *Appl. Catal. A: Gen*. **304** 178
Zhao R, Wang Y, Guo Y, Guo Y, Liu X, Zhang Z, Wang Y, Zhan W and Lu G 2006 *Green Chem*. **8** 459
Zhou L, Xu J, Miau H, Wang F and Li X 2005 *Appl. Catal. A: Gen*. **292** 223